



Study on epoxy resin-based thermal adhesive filled with hybrid expanded graphite and graphene nanoplatelet

Rajesh Kumar¹ · Smita Mohanty¹ · Sanjay K. Nayak¹

© Springer Nature Switzerland AG 2019

Abstract

Reinforced epoxy composite adhesives of expanded graphite (EG) and graphene nanoplatelet (GNPs) were prepared by hand layup and mechanical mixing method. Disk-shaped epoxy composite samples with EG and GNP mixtures in varying ratios were prepared to measure the thermal conductivity (TC) enhancement. Thermal characterization testing data showed high thermal conductivity enhancement with three different hybrid filler concentrations of 10, 25, and 35 wt%, respectively. The highest thermal conductivity of 3.6 W/m K was obtained for an epoxy adhesive composite having 30 wt.% EG and 5 wt.% GNP which was tested by guarded heat flow meter technique. This significant improvement in thermal conductivity can be attributed to the lowering of overall thermal interface resistance due to small amounts of nanofiller (GNP) improving the thermal contact between the primary microfillers (graphite). The synergistic effect of this hybrid filler system is lost at higher loadings of the GNP relative to expanded graphite. The structure of the graphite flake, GNP/epoxy, EG/epoxy and hybrid EG/GNP/epoxy composites was investigated by XRD. The EG prepared by acid intercalation and abrupt thermal expansion showed good compatibility with GNP and the epoxy resin. From scanning electron microscopy photographs, the formation of conducting network observed through the expanded graphite and GNPs in a low conducting epoxy matrix. The thermal decomposition temperature of the composite increased to 450 and 615 °C with the addition of 10 and 35 wt% of hybrid EG/GNP inside epoxy matrix, respectively. LAP shear strength of single and hybrid filled epoxy adhesive decreased at 35 wt.% loading than neat epoxy.

Keywords Thermal conductivity · Epoxy composites · Expanded graphite · Graphene nanoplatelet

1 Introduction

Now these days, an increasing trend in dimensional reduction in electronic devices has created a sequential increase in the heat dissipation issues within the electronic circuits. Thermal management is a prime importance for electronic devices to operate within their optimum temperature. Thermal interface materials (TIMs) are used to spread the heat out from the point of generation (i.e., heat source) to a heat sink by filling the air gaps which are formed during an assembly with heat producing source [1–3]. Epoxy resins have drawn attention due to their wide applications, including adhesives, coatings, structural materials, and

fiber-reinforced composites. However, they are prone to brittleness behavior and poor crack propagation resistance which restrict their application. It has some inherent thermal conductivity (~ 0.2 W/m K) and further increased by incorporation of commercially available silver, aluminum nitride, boron nitride and graphite-based micro and nanofillers by our researchers [4–6]. Many commercial thermal adhesives and pastes are available in the market. But the conductivity is not so much high. So the addition of carbon-based high conductive fillers (GNP, CNT) can provide high aspect ratio and decreased interface resistances inside epoxy resin matrix.

✉ Rajesh Kumar, rajpolymer83@gmail.com | ¹SARP-Laboratory for Advanced Research in Polymeric Materials (LARPM), Central Institute of Plastics Engineering and Technology (CIPET), B-25, Infocity Road, Patia, Bhubaneswar, Odisha 751024, India.



Expanded graphite and graphene nanoplatelets (GNPs) have a very high thermal and electrical conductivity (~ 3000 W/m K, 107 S/m). These are prepared from natural graphite flake which is abundant on earth. In graphite, each carbon is sp^2 hybridized and bonded to three other carbon atoms to form layers of hexagonal shape. These layers are joined by weak van der Waals forces which can slide over each other when force is applied. In graphite, numerous layers called as graphene are found which can be broken down and separated from graphite by different methods to separate graphene, multilayer graphene (MLG), graphene sheets, and graphene nano-platelets (GNPs) [7]. It is very difficult to separate a single layer of graphene from bulk graphite. Generally, an acid-based high oxidative intercalation method (Hammer's method) is used to break internal forces between graphene layers to extract grapheme oxide (GO); then it is further reduced or annealed to form reduced graphene oxide (rGO) which is not 100% equivalent to graphene and contains structural defects and oxide groups [8].

Further rGO shows strong interaction with each other as it is formed (due to strong intramolecular forces), as soon it comes in material contact with a support or even stacked with another graphene. The strong interactions induce a dramatic decrease in the conductivity. So, vast application of graphene-based nanocomposites is limited due to difficulties in large-scale production of graphene and their dispersion in polymer matrices. Secondly, they may irreversibly agglomerate inside the matrix and restack again through van der Waals' interactions to form graphite during the processing at higher loading of graphene, generally in the drying process. So, in situ reduction polymerization [9], coating with surfactant or functionalization is required during rGO-based composite formation to avoid agglomeration of graphene nanoparticles. These are generally used at lower filler concentration to achieve highest mechanical, thermal and electrical properties inside composites. It is generally used in high dielectric strength supercapacitor and semiconductor development [9, 10].

In general, GNPs or multi-layer graphene (MLG) can be described as graphene with more than 10 graphene layers. But graphite has comparatively more than 100 layers. Graphene nanoplatelet (GNP), with comparable properties, is an alternative type of carbon-based nanofiller. It can be produced more easily and cost-effectively in large quantities which are a stack of platelet-shaped GNSs but is still in the nanoscale in the thickness direction [11]. It has a comparatively low cost of production (compared to graphene and CNTs), light weight than metallic fillers, excellent mechanical, structural and gas barrier properties. All these properties make GNPs applicable in many engineering applications, for example in gas sensors, electromagnetic interference (EMI) shielding devices,

light emitting diodes (LEDs), fuel cells, supercapacitors and photovoltaic cells [12]. The enhanced property of reinforced GNP/epoxy composites depends on the number of stacked layers in GNP, the degree of exfoliation, its surface treatment, aspect ratio, concentration, dispersion and orientation inside the matrix. Silane functionalization of GNPs is required at a high concentration of GNP inside reinforced polymer composite to increase the interaction of GNP with polymeric chains and avoid agglomerations. Functionalization increases the mechanical strength and thermal properties, but it also generates extra interface resistances which may decrease TC due to phonon scattering at different generated interfaces [13, 14]. So the best way to increase TC of GNP-based composites is to coat or hybridize with equivalent filler having (nearly same inherent TC) which can avoid agglomeration and excess adhesion [15, 16].

Expanded graphite contains porous structure of irregularly entangled GNPs with each other due to the abrupt expansion of acid/ion intercalated graphite layers. These GNPs can be separated from EG by simple solvent-based water bath sonication method. It has an inherent thermal conductivity of nearly 1500 W/m K and contains both amorphous and crystalline regions of GNP layer units inside EG porous structure which cannot restack after composite formation due to permanent breakage of van der Waals forces [17–24]. Further, hybrid formulation of different carbon-based fillers inside reinforced polymer composites influences the size, shape and aspect ratio of fillers and produces additive or synergistic effect toward thermal conductivity enhancement of composites [11, 25–35]. In this paper, we focus our attention on expanded graphite and GNP's use in epoxy-based TIMs. GNPs were used without any further treatment or functionalization. The chosen hybrid of EG and commercial GNPs was dispersed in an industrial epoxy resin containing a reactive diluent [11, 36–43]. We claim that the choice of high aspect ratio hybrid fillers up to optimum filler loading is an important parameter to move toward adhesive composite with high thermal conductivity and a further increase in thermal conductivity of epoxy by increasing the total hybrid micro–nano-filler loading is hard to realize due to the increased filler aggregation and interfacial thermal resistance as well as dramatically increased viscosity.

2 Experimental

2.1 Raw materials

The epoxy resin (Araldite GY 250) was supplied by M/S Huntsman International (INDIA) Pvt. Ltd. It is basically, diglycidyl ether of bisphenol-A (DGEBA). It is a universal

purpose unmodified medium viscosity epoxy resin. It is suitable for the formulation of solvent-free coatings, self-leveling mortar, flooring screeds and toweling compounds etc. It has excellent mechanical properties and resistance to chemicals which can be further modified by a wide range of various hardeners and fillers. The corresponding hardener (Aradur[®] HY 951 IN) was supplied by M/S Huntsman International (INDIA) Pvt. Ltd. (mixed in a proportion of 10:1 by weight as recommended). It is basically tri-ethylene tetra amine (TETA). Epoxy reactive diluents were supplied from Marshal Polymers Pvt. Ltd., Kolkata. H_2SO_4 and HNO_3 were analytical-grade chemicals and used directly without any further purification. Graphene nanoplatelet (GNPs) were purchased from Alfa Aesar ($k \sim 2000$ W/m K). It has a thickness of 10–20 nm, the x – y dimension of 5.0 μ m and has the surface area of 500 m²/g. Expanded graphite (EG) synthesized from graphite flakes (< 20 μ m) which was supplied by Sigma-Aldrich. It has a high inherent thermal conductivity ($k \sim 1500$ W/m K) and average surface area of 400 m²/g. Graphite is the most stable form of carbon under standard condition. It is an allotrope of carbon and is a non-metallic, showing high electrical and thermal conductivity. In graphite, heat transfer takes place through phonon transfer of individual lattice units and other is the conduction of electrons through lattice units.

2.2 Preparation of expanded graphite (EG)

Raw graphite flakes were first dried in a vacuum oven for 24 h at 100 °C. Then a mixture of concentrated H_2SO_4 and HNO_3 with a volume ratio of 3:1 was added slowly to a glass flask containing required amount of anhydrous graphite flake (12 ml acid mixture for per gm graphite flake) with vigorous stirring. After 12 h of reaction, the acid-treated graphite flakes were allowed to settle down for 5 h in a 500-ml beaker. Then upper concentrated acid part was removed by pouring down inside wash basin. The remaining thick black slurry remained in beaker was diluted by adding distill water inside vacuum hood

chamber and again allowed to settle down for 5 h. After settling, the upper diluted upper part is again removed and fresh distill water is added again. Then diluted mixture was filtered (0.2-mm size PTFE membrane vacuum filtration assembly) and washed with deionised water until the pH value of the filtrate reached to 6.4. Then it was dried at 100 °C for 24 h inside hot air oven. Then small amount of dried graphite intercalation compound (GIC) was taken in a silica crucible and subjected to a thermal shock at 900 °C for 45 s inside muffle furnace for EG formation.

2.3 Fabrication of GNP, EG and hybrid EG/GNP filler-incorporated epoxy adhesives

Initially, required amount of EG, GNP and mixed EG/GNP (in 6:1 ratio) fillers powder were taken in aluminum foil and dried in vacuum oven at 100 °C for 2 h to remove any moisture. EG/epoxy, GNP/epoxy and EG/GNP/epoxy composites were prepared by mechanical mixing and in situ polymerization method. Calculated amount of epoxy and different fillers (i.e., 35, 35, 10, 25, 35 and 40 wt% of epoxy, as shown in Table 1) were added to epoxy resin contained in different mixing beakers. The reactive diluent up to 5 to 30 wt% of epoxy resin was added into mixture so that the viscosity during mixing can be minimized. It was then rotated with a mechanical mixer at 500 ± 50 rpm for one hour and further sonicated inside water bath sonicator for 3 h for proper dispersion and trapped air removal. After that 12 wt% curing agent (i.e., TETA) was added to it and mixed thoroughly for 1 min. The adhesive mixture was immediately casted inside a polypropylene mold cup of 50 mm diameter. Before casting inside the mold was cleaned by acetone and coated with wax for easy removal of cured samples. It was then allowed to cure at room temperature inside vacuum oven for 24 h. The specimen was then taken out by gentle heating and used for testing and analysis purpose. A schematic of the above sample preparation method is illustrated in Fig. 1.

Table 1 Thermal conductivity and equivalent thermal resistance (TR) of neat epoxy (Ep) and GNP, EG, hybrid EG/GNP incorporated epoxy adhesive composites

Sample name (EG/GNP at 6:1 ratio)	Filler loading (wt%)	Thermal conductivity (W/m K)	Thermal conductivity by other scientific groups (W/m K)	Equivalent thermal resistance, TR (m ² K/W $\times 10^{-3}$)
Neat epoxy (Ep)	0	0.197 ± 0.003	0.20 ± 0.01 [10]	20.3
35GNP + 65Ep	35	0.5 ± 0.007	0.65 at 10 wt% [25]	8.61
35EG + 65Ep	35	2.5 ± 0.04	4.0 at 20 wt% [17], 1.7 at 23 wt% [1]	3.77
10EG/GNP + 90Ep	10	0.5 ± 0.007	0.65 at 10 wt% [25], 0.85 at 4.5 wt% [13]	7.81
25EG/GNP + 75Ep	25	2.5 ± 0.04	1.2 at 25 wt% [32]	3.97
35EG/GNP + 65Ep	35	3.6 ± 0.054	3.5 at 37 wt% (pressed composites) [1]	1.87
40EG/GNP + 60Ep	40	3.0 ± 0.045	2.0 at 40 wt% [32]	2.55

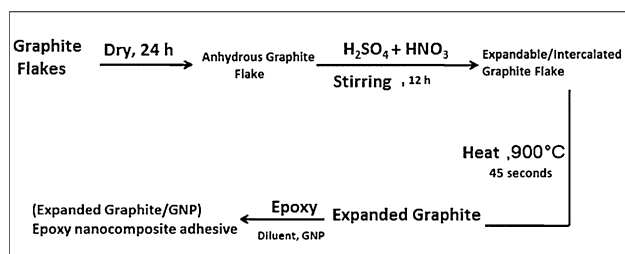


Fig. 1 Schematic representation of thermally conductive epoxy composite preparation

2.4 Characterization

XRD pattern analysis was carried out by SHIMADZU XRD-700L diffractometer, with the X-ray of 0.154 nm at diffraction of 5 degrees per minute. The thermal conductivity of neat epoxy and different filler-reinforced disk-shaped (dia 50 mm, thickness 4.5 ± 0.5 mm) epoxy composite samples was measured by steady-state guarded heat flow meter technique (ASTM E1530-06 standard) using Unitherm 2022, Anter corpo, USA. Lap shear strength of neat epoxy and different filler-incorporated epoxy adhesives was measured between single lapped aluminum substrate through Universal Testing Machine (UTM, Instron 3382, UK), according to ASTM D-1002 standard at room temperature, following pulling rate of 0.05 inch/min. Morphological study of the fracture surface of the optimized samples was carried out by scanning electron microscope (EVO MA15, Carl Zeiss SMT, Germany). Thermogravimetric analysis (TGA) was carried out by using TGA Q50, TA Instruments, USA, according to ASTM E1868 standard, and the samples were heated from 100 to 800 °C temperature at a heating rate of 10 °C/min under nitrogen purging rate of 60 ml/min.

3 Results and discussion

3.1 Structural analysis

X-ray diffraction pattern analysis (XRD) of raw graphite flake and its reinforcement inside the epoxy matrix was done to assure the graphite crystalline (graphene) lattice layer units present inside prepared epoxy adhesive composites. The XRD patterns show the different prominent peaks of raw graphite flakes, epoxy and epoxy composites which are shown in Fig. 2.

The raw graphite flake exhibits a sharp diffraction peak at a 2θ value of 26.59° and the corresponding inter-planar distance of d_{002} 3.35872 Å. It is ascribed to the highly ordered crystallographic regions present inside graphite flakes [8]. The expanded graphite exhibits a

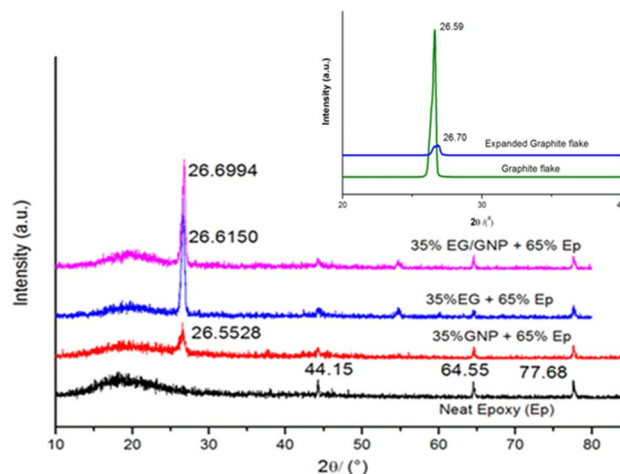


Fig. 2 XRD patterns of raw graphite flake, neat epoxy and prepared epoxy composite samples (in combination)

sharp diffraction peak at a 2θ value of 26.70° and the corresponding inter-planar distance of d_{002} 3.33556 Å. The broadening of peak occurs due to a reduction in size and disruption of the crystalline structures (amorphous regions generation) caused by the thermal exfoliation of GICs at high temperature [4]. The peaks at 2θ values of 77.68° , 64.55° , 44.15° and in the region of 13.5° – 23.5° belong to epoxy resin [7, 19]. The peaks at 2θ values of 26.5528° , 26.6150° and 26.6994° are ascribed to GNP of 35GNP + 65Ep, EG of 35EG + 65Ep and EG/GNP of 35(EG/GNP) + 65Ep composite samples and corresponding inter-planar distance of d_{002} 3.35425 Å, d_{002} 3.34655 Å, and d_{002} 3.33617 Å, respectively. XRD pattern of 35GNP + 65Ep shows peak broadening due to the smaller size of GNPs. These values of d-spacing are slightly higher than that of expanded graphite (d_{002} = 3.34162 Å) [5, 6, 44]. This is due to exfoliation and intercalation of epoxy chains between graphitic layers during mixing which increases the slight distance between graphene nanoplatelet layer units. It confirms the better interaction dispersion of EG and GNPs inside the epoxy matrix. These data are in correlation with the authors. All the above peaks of epoxy and expanded graphite (EG) are present in the epoxy composites which assure the composite formation [4, 5, 7, 9, 13].

3.2 Thermal conductivity (k)

The heat conduction is defined by the following equation:

$$Q = kA(T_1 - T_2)/t \quad (1)$$

where Q is the heat flux (W), k is the thermal conductivity (W/m K), A is the cross-sectional area (m^2), $T_1 - T_2$ is the difference in temperature (K), and t is the thickness of the sample (m).

The thermal resistance (R) of a sample can be given as

$$R = t/kA \quad (2)$$

where R is the thermal resistance (TR) of the sample between hot and cold surfaces ($\text{m}^2 \text{K/W}$).

From Eq. 2, we can write that

$$k = x/RA \quad (3)$$

Thermal conductivity test of different epoxy composite samples was determined to analyze the thermal conductivity (TC) enhancement at different single and hybrid filler loading level inside the epoxy resin. It has been proved by different authors literature work that the TC of composites based on GNPs is generally enhanced between 5 and 15 wt.% loading percentage and higher loading of GNPs decreases the optimal properties of composites [11, 13, 18]. It has also been proved that TC of EG-based composites increased between 5 and 25 wt.% loading and lesser number of scientific literature work provide TC data above 25 wt.% filler loading level. So we have taken highest loading (i.e. 35 wt.% reinforcement) percentage of these fillers inside epoxy resin to analyze the effect of these fillers at highest filler loading percentage. Several authors have optimized the hybrid filler ratio inside epoxy composites to achieve high aspect ratio of hybrid filler inside matrix for higher thermal transport mechanism. Mahanta et al. achieved a TC of 42.4 W/m K from epoxy composite filled with surface enhanced flake graphite and oxygen intercalated layer graphene, mixed in the ratio of 6:1, respectively. They have incorporated higher aspect ratio as well as functionalized hybrid fillers inside epoxy matrix to generate synergistic TC enhancement behavior. Similar type of hybrid filler mixing ratio was also taken by Zohu et al. for TC enhancement of epoxy resin [11, 22, 28]. So, we have incorporated their optimized filler mixing ratio (i.e., 6:1) inside our EG/GNP hybrid filler without having surface enhancement (i.e., functionalization) or extra chemical addition inside epoxy resin so that cost, time and excess processing can be minimized while preparing epoxy-based thermal adhesive and pastes used in electronic packaging industry. Thermal conductivities values obtained for different hybrid nanoparticle filled composite samples are shown in Table 1.

As evident from Table 1, the thermal conductivity (TC) and thermal resistance (TR) of 35GNP + 65Ep at 35 wt% GNP loading was 0.5 W/m K and $8.61 \times 10^{-3} \text{ K m}^2/\text{W}$, respectively. This is primarily due to the higher filler concentrations and high adhesion of graphene nanoparticles toward epoxy matrix which causes agglomeration of GNP sub-microparticles inside epoxy resin matrix as shown in SEM micrographs (Fig. 7) and less vibrations of phonon conducting units inside epoxy matrix take place for efficient heat transfer mechanism. This is in accordance

with Wang et al., Raza et al. and Moriche et al. who say that GNPs up to 15 wt% filler reinforcement give better TC enhancement and after that, they show self-agglomeration due to strong interaction (filler/filler interface) with each other than filler/matrix interfaces. Further functionalization or coating of GNPs is needed to achieve high interaction of GNP with epoxy polymer matrix for excess phonon transfer without scattering and efficient heat transfer mechanism at interfaces at higher filler loading percentage [11, 23–25, 27, 31].

The thermal conductivity (TC) and thermal resistance (TR) of 35EG + 65Ep sample at 35 wt% EG filler loading was 2.5 W/m K and $3.77 \times 10^{-3} \text{ K m}^2/\text{W}$, respectively. This may be due to high surface area generation and oxide functionalization of EG which avoids agglomeration of GNP layers and decreases the filler/filler interface resistances inside the epoxy matrix. This is also in accordance with reference papers [13, 17–21]. Further, incorporating hybrid fillers in increasing order up to 10 wt.%, 25 wt.%, 35 wt.% filler fraction, the thermal conductivity of EG//GNP epoxy composites were increased linearly (Fig. 3). Increase in TC for 10(EG/GNP) + 90Ep, 25(EG/GNP) + 75Ep and 35(EG/GNP) + 65Ep composite samples was 0.5 W/m K, 2.5 W/m K and 3.6 W/m K, respectively. Similarly, the TR of the above samples was marked as $7.81 \times 10^{-3} \text{ K m}^2/\text{W}$, $3.97 \times 10^{-3} \text{ K m}^2/\text{W}$ and $1.87 \times 10^{-3} \text{ K m}^2/\text{W}$, respectively. This is because of high filler concentration and high aspect ratio of fillers combination. Hybrid fillers with different ratio provide better symmetry in phonon transfer mechanism by lowering both filler–filler and filler–matrix resistances. This is in accordance with the Baruch et al., Kemaloglu et al. and Mahanta et al. They said that the aspect ratio of the filler plays important role in thermal conductivity enhancement of composite systems. A synergistic effect

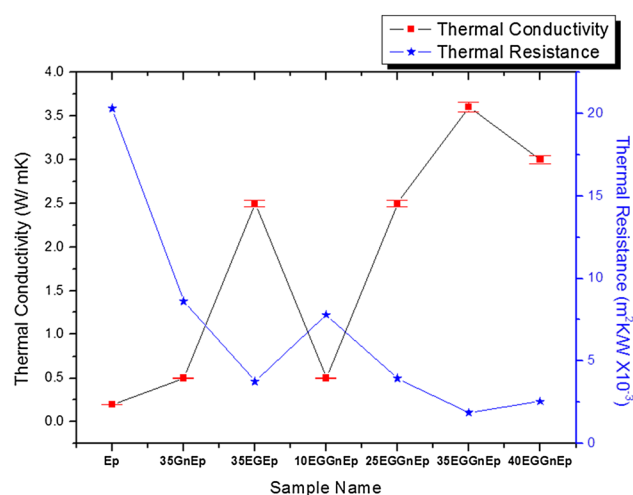


Fig. 3 Thermal conductivity and thermal resistance of different epoxy composite samples at different loading weight percentage

between the graphite nanoplatelets (GNPs) and SWCNTs in the enhancement of the thermal conductivity of epoxy composites was reported by Yu et al. and described to the formation of a more efficient percolating hybrid CNT/GNP network with significantly reduced thermal contact resistance [13, 22].

Further incorporation of hybrid fillers at 40 wt% filler fraction, the thermal conductivity of 40(EG/GNP) + 60Ep was decreased to 3.0 W/m K, consequently proclaiming the TR of $2.55 \times 10^{-3} \text{ K m}^2/\text{W}$. This is due to the synergistic effect, the high surface area and better aspect ratio of hybrid fillers inside the epoxy matrix which provide mean free path for phonon transfer without phonon scattering between filler–matrix interfaces. But at the same time increased viscosity of hybrid fillers at high concentration of filler causes the formation of voids, cracks, air bubble entrapment etc. during composite formation as shown by SEM images (Fig. 9) which causes negative effect (high phonon scattering and unavailability of shortest route path for phonon travel inside epoxy composite network) to further conductivity enhancement of hybrid epoxy composite [11, 28–30].

3.3 Morphology

Scanning electron microscopy (SEM) of raw graphite flake, expanded graphite and reinforced epoxy composites was done to analyze the presence of GNP heat conducting units and its interaction and dispersion inside the epoxy matrix. Figure 4a, b illustrates the SEM image of raw

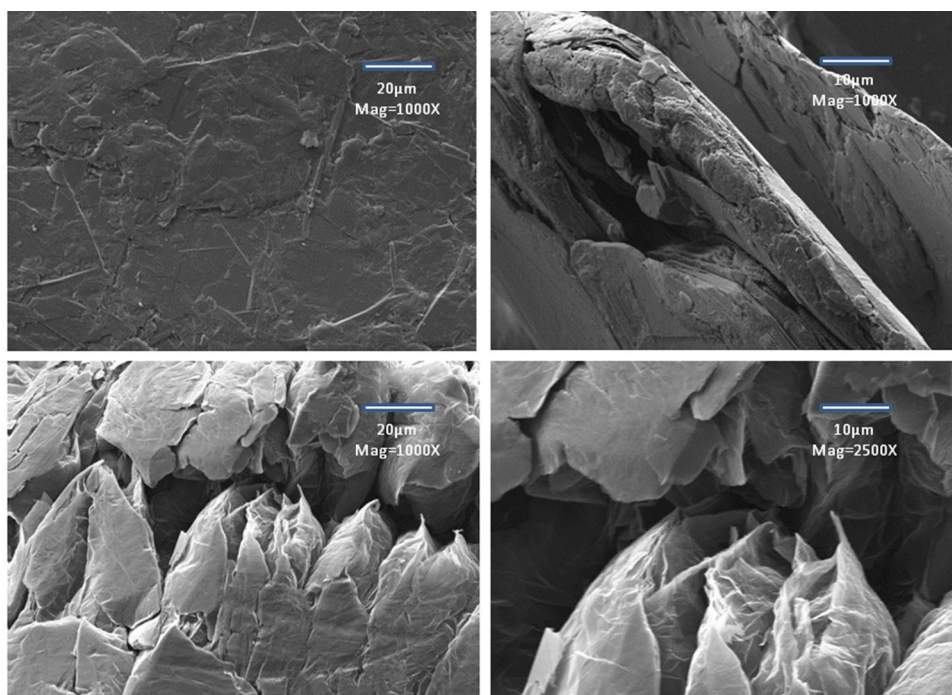
graphite flake at lower and higher magnification. It depicts that heat conducting units called as GNPs are highly compacted within each other by weak van der Waals forces, which provides very less surface area for phonon and electron conduction through GNP layers and only upper surface layers contribute in heat conduction mechanism.

Figure 4c, d shows the SEM image of expanded graphite flake after acid intercalation and thermal expansion of raw graphite flakes inside muffle furnace at 900 °C. It shows that graphene platelet layers (GNPs) are loosely intertwined and intermingled with each other during abrupt thermal expansion. They have the high number of conducting particles for heat and electricity conduction through different loose GNP unit layers [13, 17].

The microstructures of fractured epoxy composites were investigated. Neat epoxy (Fig. 5a–c) was chosen as the base to compare the microstructures of all other composites. It was difficult to scan SEM images of neat epoxy above 350× magnifications due to non-conducting nature of neat epoxy. It has been observed that the smooth surface of fractured neat epoxy composite was changed to rough surface after the incorporation of single and hybrid fillers. There were small solid lines in the region of cracks, showing brittle nature and low resistance toward propagation of stress fractures [10, 13, 44–46].

The microstructure images of impact fractured 35EG + 65Ep composite sample at a 35 wt% loading of EG are depicted in Fig. 6a. It illustrates 500X magnification image of continuously distributed expanded graphite loose layers inside epoxy matrix with some gaps,

Fig. 4 a, b SEM images of raw graphite flakes at ×1000 magnifications and c, d expanded graphite at ×1000, ×2500 magnifications, respectively



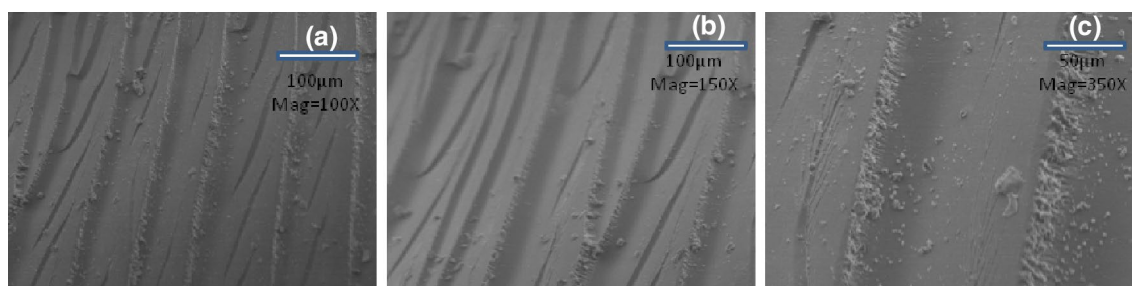
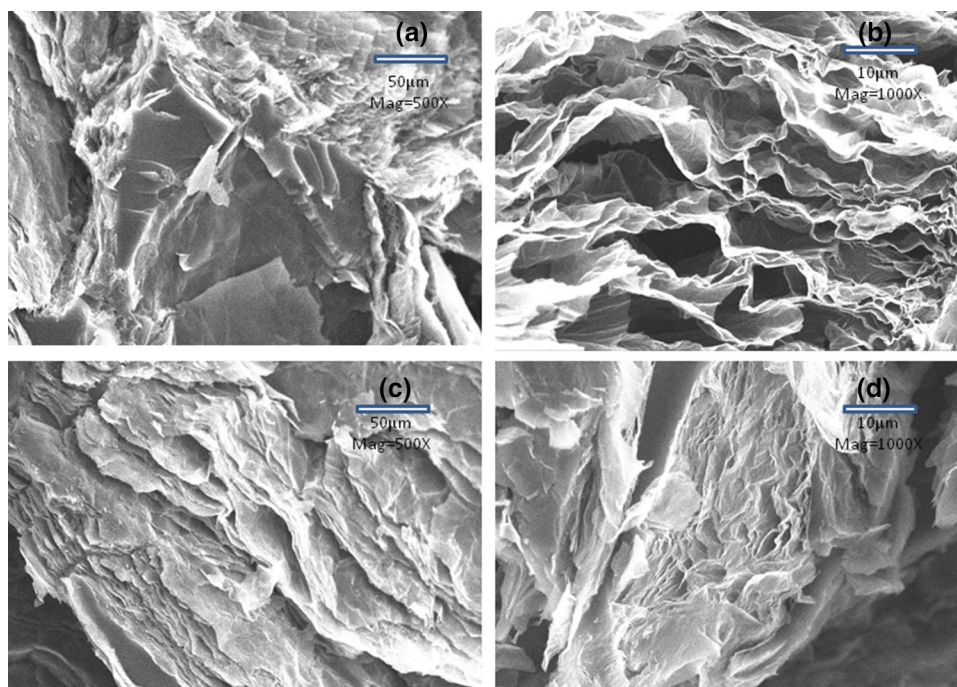


Fig. 5 SEM images of fractured surface cross section of neat epoxy (Ep)

Fig. 6 SEM images of impact fractured surface of 35EG + 65Ep composite at $\times 500$, $\times 1000$ magnifications, respectively



cracks and voids formation. Similarly Fig. 6b shows the SEM image (at 1000 \times magnification) of fractured surface which indicates good dispersion of graphite layers inside the epoxy matrix. Similarly Fig. 6c, d shows SEM images of another region at lower and higher magnification indicating that resin is continuously impregnated in between expanded graphite layers [17].

Figure 7a, b represents the microstructural images of impact fractured surface of 35GNP + 65Ep composite sample at 35 wt% loading of GNP inside epoxy. Figure 7a, b shows the strongly adhered surfaces and agglomerated regions of GNPs with an epoxy matrix which minimize the heat conduction mechanism at interfaces. Similarly, Fig. 7c, d represents the SEM images of the fractured surface at 500 \times , 1000 \times magnification which indicates that nanoscale GNPs layers show strong adhesion toward epoxy matrix phase with some cracks and air gaps [13, 25, 44–46].

Figure 8a, b represents the 50 \times and 100 \times magnified microstructural images of impact fractured surface of 10(EG/GNP) + 90Ep composite sample at 10 wt% loading of EG/GNP (6:1 ratio) inside epoxy resin. Figure 8a, b shows the randomly distributed graphite layer particles with no strong adhesion or agglomeration inside epoxy matrix which facilitate the heat conduction mechanism at interfaces. Similarly, Fig. 8c, d represents the SEM images of the fractured surface at 500 \times , 1000 \times magnification which indicates that 3D heat conductive network through graphite layers exists inside epoxy matrix phase with some cracks and air gaps presence [17, 45].

Figure 9a, b shows the microstructure images of impact fractured 40(EG/GNP) + 60Ep hybrid composite sample at 40 wt% loading of EG/GNP (i.e., 6:1 ratio). Figure 9a shows the continuously distributed channels of GNPs layer embedded in between expanded graphite and epoxy matrix which minimize the gaps between EG particles to

Fig. 7 SEM images of impact fractured surface of 35GNP + 65Ep composite sample at $\times 500$, $\times 1000$ magnifications, respectively

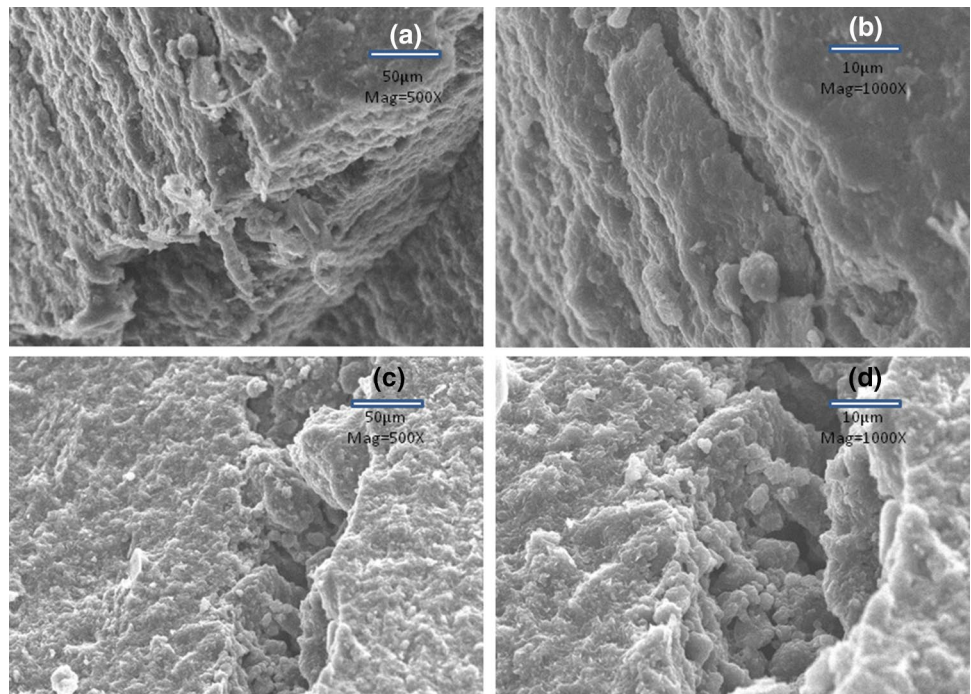
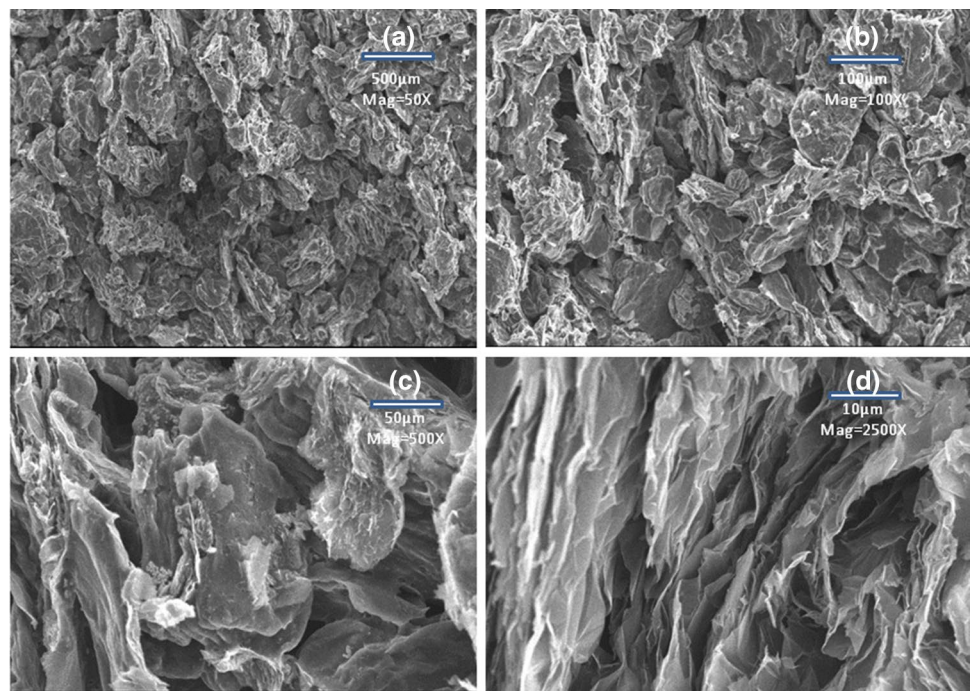


Fig. 8 SEM images of impact fractured surface of 10(EG/GNP) + 90Ep composite sample at $\times 50$, $\times 100$, $\times 500$, and $\times 1000$ magnifications, respectively



facilitate the heat conduction. Figure 9b shows the formation of heat conductive three-dimensional GNPs percolation network inside matrix for proper phonon and electron conduction through lattice vibration and electron conduction mechanism. The synergistic effect and high aspect ratio of both micro- and nanoparticles help to increase the thermal conductivity up to 3.0 W/m K. Similarly,

Fig. 9c, d represents SEM image of the fractured surface at a different region which indicates that flexible and loose bunch of GNP layers formed in between enlarged layers of expanded graphite and epoxy matrix phase which are dispersed randomly at interfaces [17, 26, 45, 46]. However, there are some agglomerations, cracks and holes presence which are formed during adhesive preparation.

Fig. 9 SEM images of impact fractured surface of 40(EG/GNP) + 60Ep composite sample at $\times 500$, $\times 1000$ magnifications, respectively

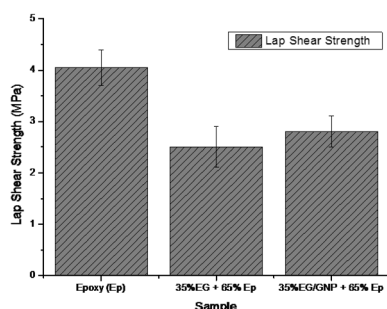
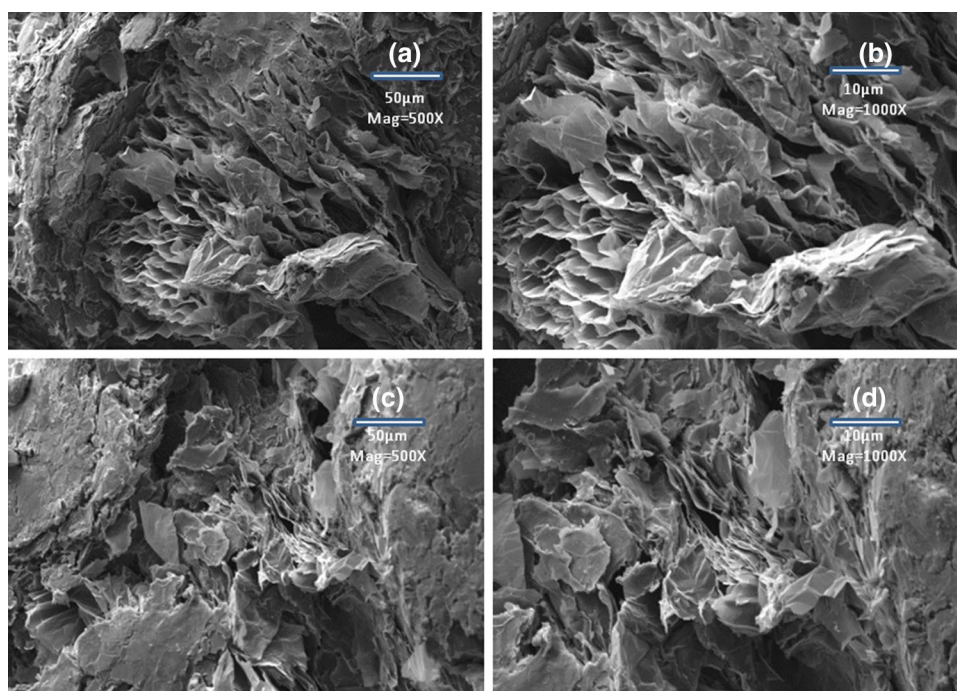


Fig. 10 Lap shear strength (LSS) of neat epoxy and hybrid epoxy adhesive at 35 wt% filler loading percentage

3.4 Lap shear strength

Lap shear strength test was done to analyze the bonding strength of prepared epoxy adhesive with an aluminum metallic surface. The lap shear strength is most essential when thermal sensor like thermocouple will be mounted to any metal substrate whose thermal activities have to be measured. So, the adhesive as well as cohesive strength

of adhesive is characterized after the surface adhesion to metallic part. The decrease in the characteristics of the filler-added epoxy is quite visible (Fig. 10).

From Table 2, it is clear that neat epoxy has higher lap shear strength (i.e., 4.05 MPa) than hybrid epoxy adhesives. Adhesive composite, 35EG + 65Ep containing 35 wt.% of EG filler inside epoxy resin showed lap shear strength of 2.5 MPa. This may be due to the porous and layered structure of expanded graphite [13]. Some microgaps also remain through which epoxy resin has not entered at higher filler loading (i.e., 35 wt%) level. So it shows lap shear strength of 2.5 MPa only and generally cohesive-type failure of bonded adhesive joint takes place during lap shear strength testing.

But the hybrid formulation of expanded graphite with GNP for 35EG/GNP + 65Ep showed slight higher lap shear strength (i.e., 2.8 MPa) than 35EG + 65Ep at same (i.e., 35 wt%) hybrid filler loading inside the epoxy resin. This is because of high adhesion strength of GNPs as shown in SEM graphs (Fig. 7) and high aspect ratio (micro and nano-hybrid formulation) inside epoxy matrix which minimizes the fill gap between EG and epoxy matrix. So it showed

Table 2 LAP shear testing data of neat epoxy and epoxy adhesive composite at 35 wt% filler loading level

Sr. No.	Sample	Lap shear strength (MPa)	Modulus (MPa)	Joint failure mode
1	Epoxy (Ep)	4.05 ± 0.35	2959 ± 395	Adhesive
2	35EG + 65Ep	2.5 ± 0.4	600 ± 50	Cohesive
3	35(EG/GNP) + 65Ep	2.8 ± 0.3	840 ± 100	Cohesive

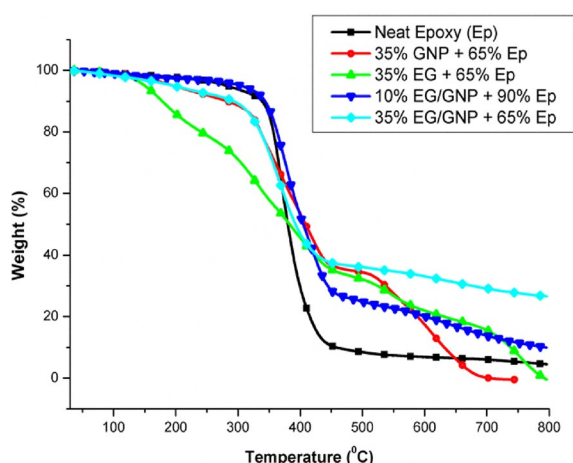


Fig. 11 Thermogravimetric analysis (TGA) thermograms of neat epoxy and epoxy adhesive composites as a function of temperature

Table 3 TGA values for neat epoxy and its composites

Sample name	T_{onset}	$T_{25\%}$	$T_{50\%}$	T_d	R_{700} (%)
Neat epoxy (Ep)	280	365	380	400	5
35GNP + 65Ep	220	350	415	535	1
35EG + 65Ep	135	260	378	510	13
10(EG/GNP) + 90Ep	300	370	415	450	12
35(EG/GNP) + 65Ep	220	350	400	615	29

more lap shear strength (LSS), and generally cohesive type of failure occurs on bonded metallic joints during lap shear strength testing [25].

3.5 Thermal properties

Thermogravimetric analysis (TGA) was performed to investigate the thermal decomposition behavior of the hybrid adhesive nanocomposite. The thermal degradation analysis of the hybrid nanocomposites was done from 30 to 800 °C, under a nitrogen atmosphere as shown in Fig. 11. The initial degradation temperature at 5% weight loss (T_{onset}), temperature at 25% weight loss ($T_{25\%}$), temperature at 50% weight loss ($T_{50\%}$), the complete decomposition temperature at 70% weight loss (T_d) and residual weight % (R_{700}) at 700 °C are presented in Table 3. Thermal stability was analyzed between 100 and 700 °C because below 100 °C, weight loss is generally due to the presence of moisture and appreciable oxidation above 700 °C. From Fig. 11, it can be seen that during thermal decomposition from 100 to 300 °C, the weight loss occurred was related to the evaporation of low molecular weight-based compounds. At this temperature, the highly volatile diluents components or moisture does exist in the adhesive in a

state of free or loosely bound water starting to evaporate [40, 48, 49].

Initial thermal degradation temperature (T_{onset}) for neat epoxy is 280 °C while those of 35GNP + 65Ep, 35EG + 65Ep, 10(EG/GNP) + 90Ep and 35(EG/GNP) + 65Ep is 220 °C, 135 °C, 300 °C and 220 °C, respectively. The data show that thermal stability of filled epoxy composite is lower than neat epoxy except for 10(EG/GNP) + 90Ep at the initial stage. This is because of non-homogenous mixing at higher filler loading percentage which increased viscosity and production of voids, gaps and large clusters. It negatively affects the extent of particle–matrix binding and decreases the thermal stability. Secondly, excessive diluent is used to lower the viscosity during mixing which decreases the cross-linking density. It produces extra non-cross-linked oligomeric epoxy chain which is more susceptible to thermal degradation at a lower temperature than neat epoxy. But in the case of 10(EG/GNP) + 90Ep composite T_{onset} is higher (delayed-type thermal degradation) than neat epoxy. This is because of proper dispersion, higher cross-linking density and higher interaction of filler units among epoxy chains without agglomeration which produce more hindering effect to heat transfer and movement in polymeric chains [36, 48, 49]. Initial stage thermal degradation of 35EG + 65Ep is much lower than 35GNP + 65Ep, 35(EG/GNP) + 65Ep and neat epoxy (Ep), respectively. We know in EG, large amorphous regions, oxide groups are present on their surfaces and GNP layers are irregularly entangled within each other due to abrupt thermal expansion. It is more difficult for epoxy resin to fully penetrate inside these units, so it creates voids, cracks and different phase formation of clustered particles inside epoxy matrix [13]. Excess reactive diluent (up to 30 wt% of epoxy) is used to lower the processing viscosity during mechanical mixing. This decreases the cross-linking density inside epoxy matrix and production of extra low molecular weight volatile compounds which expel out from the composite when heated above their melting point [32, 33]. However, in the case of 35GNP + 65Ep and 35(EG/GNP) + 65Ep in spite of having higher reactive diluent, nano size, regular shaped and high interacting particles (GNPs) are present which have more physical bonding interaction with epoxy matrix. But in the case of 10(EG/GNP) + 90Ep, synergistic interaction and reinforcement of hybrid EG/GNP with epoxy take place at lower filler concentration. In addition, low level of volatile reactive diluent is used for adhesive preparation which increases the cross-linking density inside epoxy matrix [10, 34, 36, 47, 48].

At 25% weight loss, thermal degradation temperature of neat epoxy is approx. 365 °C which is decreased to 350, 260, 350 °C for single and hybrid fillers (Table 3) except for 10(EG/GNP) + 90Ep (370 °C) due to the similar

reason mentioned above [10, 36, 49]. It seems that amorphous regions of EG and reactive diluent have a negative impact on the thermal stability of epoxy adhesive at the initial stage of temperature rise. At 50 wt% loss, the maximum thermal degradation temperature ($T_{50\%}$) of neat epoxy was 380 °C which increased to about 415, 378, 415, 400 °C for 35GNP + 65Ep, 35EG + 65Ep, 10(EG/GNP) + 90Ep and 35(EG/GNP) + 65Ep, respectively. This may be due to degradation of amorphous EG layers, increased interaction between crystalline layers of EG, evaporation of volatile reactive diluent and oligomeric epoxy chains. Degradation above this temperature mainly occurs due to pyrolysis of epoxy chains. $T_{50\%}$ of 35EG + 65Ep is slightly lower than neat epoxy because EG has higher thermal diffusivity and conductivity which aids more heat transfer to degrade epoxy chains. But in case of 35(EG/GNP) + 65Ep, $T_{50\%}$ was lower than 35GNP + 65Ep and 10(EG/GNP) + 90Ep. This may be due to high thermal conductivity and lower cross-linking density of 35(EG/GNP) + 65Ep at high filler concentration level. $T_{50\%}$ of 10(EG/GNP) + 90Ep becomes equal to 35GNP + 65Ep due to increased cross-linking density as well as higher interaction of GNPs with epoxy matrix after removal of volatile and low molecular weight compounds. At 70 wt% loss, the final thermal degradation temperature (T_d) for neat epoxy (Ep) was 400 °C which increased to 535, 510, 450 and 615 °C for 35GNP + 65Ep, 35EG + 65Ep, 10(EG/GNP) + 90Ep and 35(EG/GNP) + 65Ep, respectively. This may be due to the strong interaction of filler with remaining high molecular weight cross-linked epoxy matrix. T_d of 35GNP + 65Ep is higher than 35EG + 65Ep and 10(EG/GNP) + 90Ep because of strong adhesion of GNP with epoxy matrix and higher thermal resistance (TR) as shown in Table 1. But T_d of 35(EG/GNP) + 65Ep is much higher than all other filler formulation. This may be due to the synergistic effect of high surface area GNP layers toward interaction with expanded graphite and epoxy matrix. The residual weight (R_{700}) of neat epoxy at 700 °C was 5% which increased to 1, 13, 12 and 29% for 35GNP + 65Ep, 35EG + 65Ep, 10(EG/GNP) + 90Ep and 35(EG/GNP) + 65Ep, respectively, except 35GNP + 65Ep adhesive composite sample. The high residual mass of the composites might be due to strong interaction, compatibility and high aspect ratio of EG, and EG/GNP inside the epoxy resin. But in 35GNP + 65Ep high number of conducting GNP units exist which are more prone to thermal degradation than EG at a higher temperature. A similar type of graphene degradation behavior was observed in hybrid MWCNT/graphene-PDMS composite film by Jing et al. [36, 39–41, 47–49]. Further delayed-type thermal degradation of

35EG + 65Ep takes place at 790 °C due to appreciable oxidation leaving no residue.

4 Conclusion

Epoxy adhesive composites were prepared by reinforcement of GNPs, EG, and hybrid EG/GNPs inside the epoxy resin. The highest thermal conductivity of 3.6 ± 0.06 W/m K (~ 18 times that of the neat epoxy) was obtained for 35(EG/GNP) + 65Ep adhesive composite than all other composites. We concluded that graphene nanoplatelet (GNPs) agglomerates more inside epoxy matrix when used at a higher concentration (i.e., 35 wt%). But reinforced expanded graphite–epoxy adhesive epoxy composite has higher TC at same filler loading percentage. When EG and GNP are reinforced with hybrid formulation (at 6:1 ratio), then they show the synergistic type of thermal conductivity enhancement behavior due to the high aspect ratio, decreased filler/filler and filler/matrix interface resistances inside epoxy matrix. Lap shear strength epoxy thermal adhesives was reduced than neat epoxy at 35 wt% filler loading level due to the high viscosity of filler inside epoxy matrix. Besides the use of reactive diluent decreased the viscosity of adhesive during mechanical mixing of epoxy composites, yet it has imparted negative impact on the initial thermal degradation temperature enhancement of prepared epoxy adhesives. It indicated that the commercial use of this optimized adhesive formulation is possible for thermal interface materials (TIMs) and temperature sensor interconnection applications.

Acknowledgements This work is supported by Board of Research in Nuclear Science-BRNS (Grant No. 39/14/01/2018-BRNS/39001), Department of Atomic Energy (DAE), Govt. of India.

Compliance with ethical standards

Conflict of interest On behalf of all authors, the corresponding author states that there is no conflict of interest.

References

1. Burger N, Laachachi A, Ferriol M, Lutz M, Toniazio V et al (2016) Review of thermal conductivity in composites: mechanisms, parameters and theory. *Prog Polym Sci* 61:1–28. <https://doi.org/10.1016/j.progpolymsci.2016.05.001>
2. Alva G, Lin Y, Fang G (2018) Thermal and electrical characterization of polymer/ceramic composites with polyvinyl butyral matrix. *Mater Chem Phys* 205:401–415. <https://doi.org/10.1016/j.matchemphys.2017.11.046>
3. Anwar Z, Kausar A, Rafique I, Muhammad B (2015) Advances in epoxy/graphene nanoplatelet composite with enhanced physical properties: a review. *Polym Plast Technol Eng* 55(6):643–662. <https://doi.org/10.1080/03602559.2015.1098695>

4. Yasmin A, Daniel IM (2004) Mechanical and thermal properties of graphite platelet/epoxy composites. *Polymer* 45(24):8211–8219. <https://doi.org/10.1016/j.polymer.2004.09.054>
5. Kumar D, Singh K, Verma V, Bhatti HS (2015) Microwave assisted synthesis and characterization of graphene nanoplatelets. *Appl Nanosci* 6(1):97–103. <https://doi.org/10.1007/s13204-015-0415-9>
6. Wang Z, Luo J, Zhao G (2014) Dielectric and microwave attenuation properties of graphene nanoplatelet–epoxy composites. *AIP Adv* 4(1):017139. <https://doi.org/10.1063/1.4863687>
7. Singh AK, Panda BP, Mohanty S, Nayak SK, Gupta MK (2017) Synergistic effect of hybrid graphene and boron nitride on the cure kinetics and thermal conductivity of epoxy adhesives. *Polym Adv Technol* 28(12):1851–1864. <https://doi.org/10.1002/pat.4072>
8. Tian M, Wei Z, Zan X, Zhang L, Zhang J, Ma Q et al (2014) Thermally expanded graphene nanoplates/polydimethylsiloxane composites with high dielectric constant, low dielectric loss and improved actuated strain. *Compos Sci Technol* 99:37–44. <https://doi.org/10.1016/j.compscitech.2014.05.004>
9. Neha B, Manjula KS, Srinivasulu B, Subhas SC (2012) Synthesis and characterization of exfoliated graphite/ABS composites. *Open J Org Polym Mater* 02(04):75–79. <https://doi.org/10.4236/ojopm.2012.24011>
10. Diaz-Chacon L, Metz R, Dieudonné P, Bantignies JL, Tahir S, Hassanzadeh M et al (2015) Graphite nanoplatelets composite materials: role of the epoxy-system in the thermal conductivity. *J Mater Sci Chem Eng* 3(05):75. <https://doi.org/10.4236/msce.2015.3500>
11. Zhou T, Wang X, Cheng P, Wang T, Xiong D, Wang X (2013) Improving the thermal conductivity of epoxy resin by the addition of a mixture of graphite nanoplatelets and silicon carbide microparticles. *Express Polym Lett* 7(7):585–594. <https://doi.org/10.3144/expresspolymlett.2013.56>
12. Shtein M, Nativ R, Buzaglo M, Regev O (2015) Graphene-based hybrid composites for efficient thermal management of electronic devices. *ACS Appl Mater Interfaces* 7(42):23725–23730. <https://doi.org/10.1021/acsami.5b07866>
13. Sun R, Yao H, Zhang HB, Li Y, Mai YW, Yu ZZ (2016) Decoration of defect-free graphene nanoplatelets with alumina for thermally conductive and electrically insulating epoxy composites. *Compos Sci Technol* 137:16–23. <https://doi.org/10.1016/j.compscitech.2016.10.017>
14. Wang F, Drzal LT, Qin Y, Huang Z (2015) Effects of functionalized graphene nanoplatelets on the morphology and properties of epoxy resins. *High Perform Polym* 28(5):525–536. <https://doi.org/10.1177/0954008315588983>
15. Chiguma J, Johnson E, Shah P, Gornopolskaya N, Jones WE Jr (2013) Thermal diffusivity and thermal conductivity of epoxy-based nanocomposites by the laser flash and differential scanning calorimetry techniques. *Open J Compos Mater* 03(03):51–62. <https://doi.org/10.4236/ojcm.2013.33007>
16. Liem H, Choy HS (2013) Superior thermal conductivity of polymer nanocomposites by using graphene and boron nitride as fillers. *Solid State Commun* 163:41–45. <https://doi.org/10.1016/j.ssc.2013.03.024>
17. Debelak B, Lafdi K (2007) Use of exfoliated graphite filler to enhance polymer physical properties. *Carbon* 45(9):1727–1734. <https://doi.org/10.1016/j.carbon.2007.05.010>
18. Fukushima H, Drzal LT, Rook BP, Rich MJ (2006) Thermal conductivity of exfoliated graphite nanocomposites. *J Therm Anal Calorim* 85(1):235–238. <https://doi.org/10.1007/s10973-005-7344-x>
19. Gantayat S, Prusty G, Rout DR, Swain SK (2015) Expanded graphite as a filler for epoxy matrix composites to improve their thermal, mechanical and electrical properties. *New Carbon Mater* 30(5):432–437. [https://doi.org/10.1016/s1872-5805\(15\)60200-1](https://doi.org/10.1016/s1872-5805(15)60200-1)
20. Yu A, Ramesh P, Itkis ME, Bekyarova E, Haddon RC (2007) Graphite nanoplatelet–epoxy composite thermal interface materials. *J Phys Chem C* 111(21):7565–7569. <https://doi.org/10.1021/jp071761s>
21. Drzal LT, Fukushima H (2006) Exfoliated graphite nanoplatelets (xGNP): a carbon nanotube alternative. In: *Proceedings of NSTI nanotechnology conference and trade show*
22. Mahanta NK, Loos MR, Manas Zloczower I, Abramson AR (2015) Graphite–graphene hybrid filler system for high thermal conductivity of epoxy composites. *J Mater Res* 30(07):959–966. <https://doi.org/10.1557/jmr.2015.68>
23. Wang F, Drzal LT, Qin Y, Huang Z (2014) Mechanical properties and thermal conductivity of graphene nanoplatelet/epoxy composites. *J Mater Sci* 50(3):1082–1093. <https://doi.org/10.1007/s10853-014-8665-6>
24. Raza MA, Westwood AVK, Stirling C (2012) Effect of processing technique on the transport and mechanical properties of graphite nanoplatelet/rubbery epoxy composites for thermal interface applications. *Mater Chem Phys* 132(1):63–73. <https://doi.org/10.1016/j.matchemphys.2011.10.052>
25. Moriche R, Prolongo SG, Sánchez M, Jiménez-Suárez A, Chamizo FJ, Ureña A (2016) Thermal conductivity and lap shear strength of GNP/epoxy nanocomposites adhesives. *Int J Adhes Adhes* 68:407–410. <https://doi.org/10.1016/j.jadhadh.2015.12.012>
26. Raza MA, Westwood A, Stirling C (2015) Comparison of carbon nanofiller-based polymer composite adhesives and pastes for thermal interface applications. *Mater Des* 85:67–75. <https://doi.org/10.1016/j.matdes.2015.07.008>
27. Cui T, Li Q, Xuan Y, Zhang P (2015) Preparation and thermal properties of the graphene–polyolefin adhesive composites: application in thermal interface materials. *Microelectron Reliab* 55(12):2569–2574. <https://doi.org/10.1016/j.microrel.2015.07.036>
28. Kim HS, Kim JH, Yang CM, Kim SY (2017) Synergistic enhancement of thermal conductivity in composites filled with expanded graphite and multi-walled carbon nanotube fillers via melt-compounding based on polymerizable low-viscosity oligomer matrix. *J Alloys Compd* 690:274–280. <https://doi.org/10.1016/j.jallcom.2016.08.141>
29. Fu YX, He ZX, Mo DC, Lu SS (2014) Thermal conductivity enhancement of epoxy adhesive using graphene sheets as additives. *Int J Therm Sci* 86:276–283. <https://doi.org/10.1016/j.jithe.2014.07.011>
30. Shtein M, Nativ R, Buzaglo M, Kahil K, Regev O (2015) Thermally conductive graphene–polymer composites: size, percolation, and synergy effects. *Chem Mater* 27(6):2100–2106. <https://doi.org/10.1021/cm504550e>
31. Khan MO, Leung SN, Chan E, Naguib HE, Dawson F, Adinkrah V (2013) Effects of micro-sized and nano-sized carbon fillers on the thermal and electrical properties of polyphenylene sulfide based composites. *Polym Eng Sci* 53(11):2398–2406. <https://doi.org/10.1002/pen.23503>
32. Zhou S, Chen Y, Zou H, Liang M (2013) Thermally conductive composites obtained by flake graphite filling immiscible Polyamide 6/Polycarbonate blends. *Thermochim Acta* 566:84–91. <https://doi.org/10.1016/j.tca.2013.05.027>
33. Du L, Jana SC (2007) Highly conductive epoxy/graphite composites for bipolar plates in proton exchange membrane fuel cells. *J Power Sources* 172(2):734–741. <https://doi.org/10.1016/j.jpowsour.2007.05.088>
34. Ciecierska E, Boczkowska A, Kurzydowski KJ, Rosca ID, Van Hoa S (2012) The effect of carbon nanotubes on epoxy matrix nanocomposites. *J Therm Anal Calorim* 111(2):1019–1024. <https://doi.org/10.1007/s10973-012-2506-0>
35. Choi S, Yang J, Kim Y, Nam J, Kim K, Shim SE (2014) Microwave-accelerated synthesis of silica nanoparticle-coated graphite

- nanoplatelets and properties of their epoxy composites. *Compos Sci Technol* 103:8–15. <https://doi.org/10.1016/j.compscitech.2014.08.003>
36. Kumar K, Ghosh PK, Kumar A (2016) Improving mechanical and thermal properties of TiO₂-epoxy nanocomposite. *Compos Part B Eng* 97:353–360. <https://doi.org/10.1016/j.compositesb.2016.04.080>
37. Kim K, Kim J (2016) BN-MWCNT/PPS core-shell structured composite for high thermal conductivity with electrical insulating via particle coating. *Polymer* 101:168–175. <https://doi.org/10.1016/j.polymer.2016.08.062>
38. Zhou J, Jiang Y, Wu G, Wu W, Wang Y, Wu K, Cheng Y (2017) Investigation of dielectric and thermal conductive properties of epoxy resins modified by core-shell structured PS@SiO₂. *Compos Part A Appl Sci Manuf* 97:76–82. <https://doi.org/10.1016/j.compositesa.2017.03.005>
39. Yang X, He W, Wang S, Zhou G, Tang Y (2011) Preparation and properties of a novel electrically conductive adhesive using a composite of silver nanorods, silver nanoparticles, and modified epoxy resin. *J Mater Sci Mater Electron* 23(1):108–114. <https://doi.org/10.1007/s10854-011-0485-8>
40. Parimalam M, Islam MR, Yunus RM (2018) Effects of nanosilica, zinc oxide, titanium oxide on the performance of epoxy hybrid nanocoating in presence of rubber latex. *Polym Testing* 70:197–207. <https://doi.org/10.1016/j.polymertesting.2018.07.00>
41. Yan J, Jeong YG (2015) Synergistic effect of hybrid carbon fillers on electric heating behavior of flexible polydimethylsiloxane-based composite films. *Compos Sci Technol* 106:134–140. <https://doi.org/10.1016/j.compscitech.2014.11.016>
42. Li Y, Li B, Chen W (2014) A study on the reactive diluent for the solvent-free epoxy anticorrosive coating. *J Chem Pharm Res* 6(7):2466–2469
43. Inoue M, Liu J (2008) Electrical and thermal properties of electrically conductive adhesives using a heat-resistant epoxy binder. In: 2nd electronics system integration technology conference. <https://doi.org/10.1109/estc.2008.4684514>
44. Guan LZ, Wan YJ, Gong LX, Yan D, Tang LC, Wu LB, Jiang JX, Lai GQ (2014) Toward effective and tunable interphases in graphene oxide/epoxy composites by grafting different chain lengths of polyetheramine onto graphene oxide. *J Mater Chem A* 2(36):15058–15069. <https://doi.org/10.1039/c4ta02429j>
45. Zang J, Wan YJ, Zhao L, Tang LC (2015) Fracture behaviors of TRGO-filled epoxy nanocomposites with different dispersion/interface levels. *Macromol Mater Eng* 300(7):737–749. <https://doi.org/10.1002/mame.201400437>
46. Tang LC, Wan YJ, Yan D, Pei YB, Zhao L, Li YB, Wu LB, Jiang JX, Lai GQ (2013) The effect of graphene dispersion on the mechanical properties of graphene/epoxy composites. *Carbon* 60:16–27. <https://doi.org/10.1016/j.carbon.2013.03.050>
47. Wan YJ, Tang LC, Gong LX, Yan D, Li YB, Wu LB, Jiang JX, Lai GQ (2014) Grafting of epoxy chains onto graphene oxide for epoxy composites with improved mechanical and thermal properties. *Carbon* 69:467–480. <https://doi.org/10.1016/j.carbon.2013.12.050>
48. Wan YJ, Tang LC, Yan D, Zhao L, Li YB, Wu LB, Jiang JX, Lai GQ (2013) Improved dispersion and interface in the graphene/epoxy composites via a facile surfactant-assisted process. *Compos Sci Technol* 82:60–68. <https://doi.org/10.1016/j.compscitech.2013.04.009>
49. Gong LX, Zhao L, Tang LC, Liu HY, Mai YW (2015) Balanced electrical, thermal and mechanical properties of epoxy composites filled with chemically reduced graphene oxide and rubber nanoparticles. *Compos Sci Technol* 121:104–114. <https://doi.org/10.1016/j.compscitech.2015.10.023>

Publisher's Note Springer Nature remains neutral with regard to jurisdictional claims in published maps and institutional affiliations.